Acceleration of Electron−Transfer−Induced Fluorescence Quenching upon Conversion to the Signaling State in the Blue−Light Receptor, TePixD, from Thermosynechococcus elongatus

ARTICLE *in* THE JOURNAL OF PHYSICAL CHEMISTRY B · JUNE 2009

Impact Factor: 3.3 · DOI: 10.1021/jp901631b · Source: PubMed

Acceleration of Electron-Transfer-Induced Fluorescence Quenching upon Conversion to the Signaling State in the Blue-Light Receptor, TePixD, from *Thermosynechococcus elongatus*

Yutaka Shibata,*,† Yoshiya Murai,† Yosuke Satoh,† Yoshimasa Fukushima,† Koji Okajima,‡ Masahiko Ikeuchi,§ and Shigeru Itoh†

Division of Material Science (Physics), Graduate School of Science, Nagoya University, Nagoya 464-8602, Japan, Department of Biological Science, Graduate School of Science, Osaka Prefecture University, 1-1 Gakuen-cho, Sakai, Osaka 599-8531, Japan, and Department of Life Science, Graduate School of Arts and Sciences, University of Tokyo, Tokyo 153-8902, Japan

Received: February 22, 2009; Revised Manuscript Received: April 19, 2009

TePixD is a blue light using flavin (BLUF) protein of a thermophilic cyanobacterium, *Thermosynechococcus elongatus*. The fluorescence dynamics of TePixD was observed for the first time in both its dark-adapted and signaling (red-shifted) forms with a 200-fs time resolution. The fluorescence up-conversion setup was used in the time region up to 60 ps, and the streak-camera setup was used in the time region up to 1 ns. To avoid the accumulation of the red-shifted form by the exciting laser irradiation, the sample solution was circulated using a diaphragm pump. A handmade flow cuvette with a small cross section was used to achieve a fast flow of the solution in the excited region. The fluorescence decay times were unequivocally determined to be 13.6 and 114 ps for the dark-adapted form and 1.37 ps for the red-shifted form. The double-exponential fluorescence decay in the dark-adapted form suggested the coexistence of two conformations that have the 13.6- and 114-ps decay components, respectively. The single-exponential fluorescence decay in the red-shifted form suggested the elimination of heterogeneity in the conformation upon the light-induced conversion. The fast fluorescence-quenching components were almost eliminated in the mutant in which the conserved tyrosine Tyr8 is replaced by phenylalanine. Thus, the fluorescence quench was concluded to arise from the electron transfer from Tyr8, to the excited flavin chromophore. The 10-fold-faster quenching in the red-shifted form suggested the acceleration of the electron transfer. The faster decay time of 13.6 ps for the dark-adapted form was found to be almost temperature independent in the region from 10 to 40 °C. This suggested that the energy gap, ΔG, in Marcus's electron-transfer theory is optimized to give the fastest rate. The acceleration of the electron transfer in the red-shifted form is interpreted to be due to the enhancement of the electronic-coupling factor between the donor and acceptor. A shortening of the Tyr8−flavin distance by 1.0−1.5 Å was suggested if we adopt the empirical formula for the donor−acceptor distance dependence of the electron transfer rate.

I. Introduction

Flavin is a ubiquitously distributed cofactor of proteins. Its potential ability for various chemical reactions such as electron transfer (ET) and proton transfer underlies a wide variety of activities of flavoproteins. The photochemistry after the blue-light absorption has been known to be one of the important functions of flavin in some photoreceptor proteins[1−3] or DNA-repairing enzymes.[4,5] Genomic analyses over the past decade have revealed several novel classes of light-sensing proteins using flavin as a photoreceptor pigment. Blue-light sensing using FAD (BLUF), a flavin-binding photoreceptor domain, was discovered as the N-terminal part of the flavoprotein AppA from the purple bacterium *Rhodobacter sphaeroides*.[1,6] A BLUF domain noncovalently binds flavin adenine dinucleotide (FAD) as its photoreceptor pigment.

The signaling state of a BLUF domain has been characterized by the 10−15-nm red shift of the absorption spectrum of FAD.[1,7−13] FTIR and Raman spectroscopies showed that the light-induced reaction to the signaling state (hereafter designated as a red-shifted form) results in the 10-cm^{-1} red shift of the stretching mode of the C4═O carbonyl group of FAD.[8,14−16] The formation of the red-shifted form has been considered to be caused by the modified hydrogen-bonding network surrounding FAD without any change in the covalent bonds of the chromophore. This contrasts with the known mechanisms of the photoreactions of the other flavin-binding photoreceptors. For example, in an LOV domain, a covalent adduct is known to be formed between the flavin and the cysteine residue upon conversion to the signaling state.[17,18] The red-shifted form of BLUF is rather stable and shows a long recovery time to the dark-adapted state ranging from ca. 30 s in the cyanobacterial BLUF domain, PixD,[12,19] to ca. 20 min in AppA.[1]

Gauden et al. revealed the kinetics of the initial photoreaction of SyPixD, which is a BLUF protein of the cyanobacterium *Synechocystis PCC6803*, using the ultrafast transient-absorption technique.[20] The results suggested the formation of the anion-radical and neutral-radical states of FAD before the red shift of its absorption spectrum within 65 ps. They proposed a model of the initial photoreaction of SyPixD based on their observations. The key processes assumed in the model are successive charge separation and charge recombination between the

* Corresponding author. Fax: 81-52-789-2883. E-mail: yshibata@bio.phys.nagoya-u.ac.jp.
† Nagoya University.
‡ Osaka Prefecture University.
§ University of Tokyo.

10.1021/jp901631b CCC: $40.75
Published on Web 05/18/2009

conserved tyrosine (Tyr) residue and FAD, which modify the hydrogen-bond network around FAD and induce the red-shifted form. Gauden et al. considered that the rearrangement of the hydrogen-bond network is mainly induced by the flip of Gln50. Analyses of the site-directed mutations for SyPixD and TePixD from a thermophilic cyanobacterium, *Thermosynechococcus elongatus* (*T. elongatus*), showed the indispensable role of the conserved Tyr8 residue for the formation of the red-shifted form.[11,16,21] The conserved Gln50 residue was also found to be indispensable for the photoreaction. These results are basically consistent with the reaction model by Gauden et al.

Recently, Sadeghian et al. conducted a quantum mechanics/molecular mechanics (QM/MM) simulation to elucidate the mechanism of the initial photoreaction of a BLUF protein.[22] They proposed a model in which the key role of the primary ET and the following charge recombination was basically the same as that in the model of Gauden et al. However, the conserved Gln residue was postulated not to be flipped but, rather, converted to its tautomeric form. Domratcheva et al. originally proposed the transient conversion of the Gln residue to its tautomeric form after the initial photoreaction of flavin.[23] The model of Sadeghian et al. emphasized the importance of the flip of the conserved Asp residue rather than of that of the Gln residue in altering the hydrogen-bond network. Their study also suggested that the primary photochemistry in a BLUF protein occurs through the conical intersection mechanism.

As shown above, it is widely accepted that the initial photochemistry of a BLUF protein is triggered by the successive charge separation and recombination between the flavin chromophore and nearby conserved Tyr residue. This interpretation, originally proposed for SyPixD, has been considered generally applicable to all BLUF proteins. The initial charge-separation rate was estimated to be 7 ps for SyPixD.[24] On the other hand, the rate for AppA was estimated to be 90 ps in the dark-adapted form and shown to be accelerated up to 7 ps in its red-shifted form.[25] It is not clear what causes the wide diversity in the primary ET rate among different BLUF proteins and different forms in spite of their very similar structures around the FAD as determined by X-ray crystallographic studies.[11,26−28] Toh et al. gave a tentative explanation for this in the framework of Marcus's theory of ET.[29]

Here, we studied the ultrafast fluorescence-quenching dynamics of TePixD using the fluorescence up-conversion technique. There have been several reports about the time-resolved-fluorescence measurements of BLUF proteins with limited time resolutions.[12,13,24,30,31] There have been also reports about the time-resolved fluorescence observations using the femtosecond fluorescence up-conversion method for AppA.[32,33] Here, the fluorescence dynamics was observed with a 200-fs time resolution for the first time in both the dark-adapted ($TePixD_D$) and red-shifted ($TePixD_{red}$) forms. Since a fluorescence time profile directly reflects the time dependence of the excited-state population, its interpretation is rather straightforward. In contrast, the interpretation of a transient-absorption measurement often requires intense analysis procedures, such as target analysis. The information about the ultrafast fluorescence dynamics can thus be complementary to that of the transient absorption. In the fluorescence up-conversion method, a high excitation power is required to obtain sufficient signal intensity. In order to avoid the photoaccumulation of $TePixD_{red}$ in the excited volume, we caused the rapid circulation of the sample solution by using a diaphragm pump and handmade flow cuvette. We measured the fluorescence dynamics of the same sample in the nanosecond time region and used the streak-camera setup. The combination of the data of the two experimental setups enabled us to obtain the fluorescence dynamics over a very wide time range from femtoseconds to nanoseconds.

The results clearly showed a somewhat slower primary ET rate for $TePixD_D$ than that for SyPixD in the dark-adapted form ($SyPixD_D$) and a surprisingly faster ET rate in $TePixD_{red}$ than in $TePixD_D$. In order to determine whether the redox potentials of the conserved Tyr8 (donor) and FAD (acceptor) are optimized for the primary ET reaction, we explored the temperature dependence of the fluorescence decay time in the 10−40 °C temperature region. Marcus's theory predicts that the rate of the ET reaction becomes temperature independent when the redox potentials of the donor and acceptor are optimized.[29] Furthermore, the fluorescence dynamics were compared among various TePixD mutants in which the conserved Tyr8 and Gln50 residues were replaced. The substituted phenylalanine in the Tyr8Phe mutant cannot be an electron donor to FAD. The mutations at Gln50 modify the conformation of Ty8 that is hydrogen-bonded to Gln50 in the wild-type protein. The previous studies have shown that all of these TePixD mutants lost their ability for light-induced conversion to the red-shifted form at room temperature.[16] At 80 K, a partially red-shifted form could be formed in the Tyr8 mutant but not in the Gln50 mutant.[21] The origin of the diversity in the primary ET rates in various BLUF proteins will be discussed.

II. Experimental Methods

The cloning, expression, and purification of the wild-type and mutant TePixD's of *T. elongatus* were conducted as described previously[16,21] with minor modifications. Briefly, DNA of the wild-type and mutant TePixD's was inserted into the pET28a vector (Novagen) to allow the expression with an N-terminal $(His)_6$ tag. The proteins were expressed in *Escherichia coli* BL21 (DE3) pLysS with the recombinant plasmids in the presence of 20 μg/mL Kanamycin at 37 °C for 18 h. Harvested cells were treated by the freeze−thaw procedure and disrupted using a French-pressure cell in the presence of 1 M NaCl. The elution was centrifuged at 30000*g* at 4 °C for 1 h, and the His-tagged proteins were purified from the supernatant using nickel-affinity column chromatography (HiTrap Chelating HP; Amersham Biosciences, Piscataway, NJ). The purified proteins were dissolved in a 20 mM HEPES (pH 7.5) buffer containing 1 M NaCl.

To control the amount of the photoaccumulation of the red-shifted form in the excited region, the sample solution was circulated with various flow rates. A peristaltic pump (SJ-1211H; Atto, Tokyo) was used in the flow-rate region of 0−15 mL/min, and a diaphragm pump (NF300; KNF Japan, Tokyo) was used in the flow-rate region of 360−900 mL/min. To achieve a fast flow velocity of the solution at the excited position, we used a handmade glass flow cuvette having a small square-shaped cross section of the flow path. The cross section of the flow path was a 1 mm/side square, and the flow velocity reached 12 m/s when the flow rate was 720 mL/min. Approximately 200 mL of the sample solution was circulated and the reservoir was immersed in a crushed-ice bath. The temperature of the sample in the reservoir was about 10 °C in this case. For measurements at higher temperatures, the reservoir was immersed in a temperature-controlled water bath. We confirmed that the sample was not damaged even after continuous circulation for several hours by checking the absorption spectrum.

A Ti:sapphire laser (MaiTai; Spectra-Physics, Mountain View, CA) with a repetition rate of 80 MHz was used as the

excitation source for both the fluorescence up-conversion and streak-camera setups. The sample was excited by the frequency-doubled output at 430 nm, which is the peak wavelength of the absorption spectrum of the $TePixD_D$. The excitation laser was passed through a $\lambda/2$ plate to control its polarization direction. The excitation-laser power was 6 mW (75 pJ/pulse). The beam diameter at the focal plane was roughly estimated to be 40 μm, and the excitation power per unit area was ca. 500 W/cm^2.

The fluorescence from the sample was collimated by an off-axis paraboloidal mirror and passed through a long-pass filter (Y-45; Toshiba, Tokyo). In the fluorescence up-conversion setup, the collimated fluorescence beam was focused to a type I BBO crystal (thickness 0.5 mm) by another paraboloidal mirror. The up-conversion light generated on the crystal was passed through a prism, focused on the 10-cm monochromator (CT-10, 300 g/mm; JASCO, Tokyo) for wavelength selection, and detected by a photomultiplier (R4220; Hamamatsu Photonics, Inc., Hamamatsu). In the streak-camera measurement, the collimated fluorescence beam was reflected by a flat mirror and focused on the entrance slit of the polychromator (Chromex 2501-S; Hamamatsu Photonics, Inc., Hamamatsu) connected to the streak-camera head (C4334; Hamamatsu Photonics, Inc., Hamamatsu). The full width at half-maximums (fwhm's) of the instrumental response functions (IRFs) were 210 fs and 83 ps for the up-conversion and streak-camera setups, respectively.

The wavelength-dependent sensitivity of the streak-camera system was corrected by measuring the emission spectrum of a standard lamp. Owing to the shared optical configurations of the excitation and collection of the fluorescence by the up-conversion and streak-camera setups, the sensitivity-corrected time-resolved-fluorescence spectrum could be obtained over a wide temporal range from 10 fs to 10 ns through the global analysis of the data obtained from the two setups.

III. Results

A. Flow-Rate Dependence of the Fluorescence Decay Kinetics of the Wild-Type TePixD. Figure 1 shows the fluorescence dynamics of TePixD at 500 nm observed by the up-conversion (A) and streak-camera (B) setups. The flow rate was 360 mL/min, and the excitation wavelength was at 430 nm. This flow rate results in a predominant population in $TePixD_D$ as shown later. The fluorescence dynamics in Figure 1 were observed in the magic-angle polarizer configurations. We also measured the fluorescence polarization anisotropies, which took a value of ca. 0.4 over the whole time range (data not shown). This suggests that no rotational diffusion takes place in the observed time region. The solid lines in panels A and B in Figure 1 show the fitting curves to the sum of four exponentials convolved with Gaussian IRFs with fwhm's of 210 fs and 83 ps, respectively. The fittings were performed globally so that the amplitudes and decay times would take the same values between the fitting curves to the data obtained by the up-conversion and streak-camera setups. The model curves accurately reproduced the data obtained from both setups. The decay times were estimated to be 1.4 ps, 14 ps, 110 ps, and 2.0 ns.

The scattered dots in Figure 2 show the fluorescence decays of TePixD at 500 nm in the magic-angle configuration with various flow rates. The decay time of the fluorescence was clearly flow rate dependent. It became slower upon the acceleration of the flow rate. This shows that $TePixD_D$, which accumulates with a fast flow rate, shows a slower fluorescence decay than $TePixD_{red}$. The solid lines in Figure 2 are the fitting curves to the sum of the exponential decays convolved with a

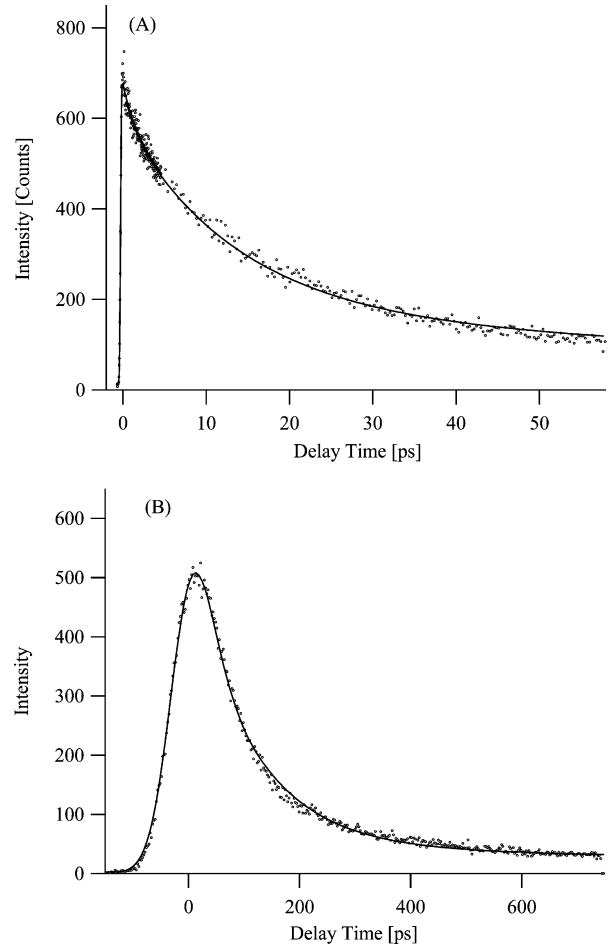

Figure 1. Time courses (circles) of the fluorescence of TePixD at 500 nm observed using the fluorescence up-conversion (A) and streak-camera (B) setups. The solid lines in (A) and (B) show the fitting curves to the decay curves of the magic-angle configuration.

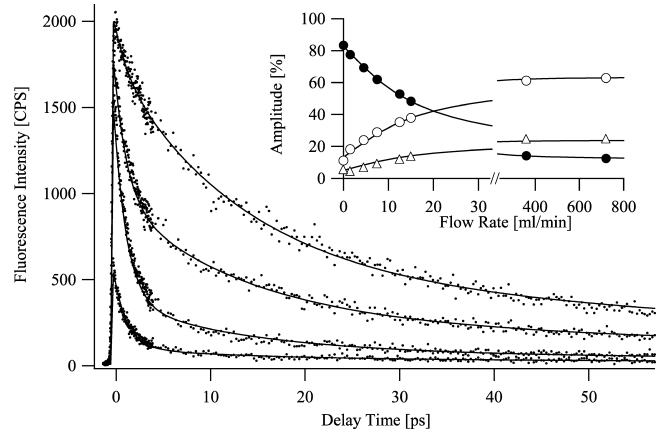

Figure 2. Fluorescence decay curves (scattered dots) in the magic-angle configuration of TePixD observed by the fluorescence up-conversion setup at 500 nm with various flow rates. The flow rate was 360 (top curve), 15, 1.5, and 0 mL/min (bottom curve). The solid lines show the fitting curves to the sum of three exponential functions. The inset shows the flow-rate dependences of the fractional ratios of the decay components with time constants of 1.37 (closed circles), 13.6 (open circles), and 114 ps (open triangles). The solid lines in the inset show the fittings. See text for details.

Gaussian IRS. Here, the fitting was performed globally so that the decay times would take the same values among the data with different flow rates while the amplitudes were freely varied. A sum of three exponentials with time constants of 1.37 ps,

13.6 ps, and 114 ps could accurately reproduce the observed data over the whole flow-rate range, as shown in Figure 2. The contribution of the slow component with a time constant of 2.0 ns was negligible, and it was omitted in the fitting to the data in Figure 2.

The Figure 2 inset shows the flow-rate dependence of the amplitude of each decay component obtained from the above fitting. The amplitude of the fastest component with a decay time of 1.37 ps decreased, while those of the slower two components with time constants of 13.6 and 114 ps increased upon the acceleration of the flow rate. Thus, we assigned the former component as originating from $TePixD_{red}$ and the latter ones from $TePixD_D$. The population ratios of $TePixD_D$, n_D, and $TePixD_{red}$, n_{red}, in the excited volume can be expressed as

$$n_{red} = \frac{1}{l}\int_0^l \exp(-k_{exc}\Phi x/v)\,dx = \frac{v}{k_{exc}l\Phi}\left[1 - \exp\left(-\frac{k_{exc}l\Phi}{v}\right)\right] \quad (1)$$

$$n_D = 1 - n_{red} = 1 - \frac{v}{k_{exc}l\Phi}\left[1 - \exp\left(-\frac{k_{exc}l\Phi}{v}\right)\right] \quad (2)$$

Here l is the length of the excited volume along the flow direction, k_{exc} is the rate of the excitation by the laser, and Φ is the quantum yield of the photoreaction. v is the flow velocity [cm/s] of the molecules in the excited volume and is related to the flow rate f [mL/min] as $v = f/60S$, where S is the cross-sectional area of the flow path (0.01 cm^2 in the present experiment).

The solid lines in the Figure 2 inset are the fitting curves based on eqs 1 and 2. The fitting curves contain the correction terms to express the residual $TePixD_{red}$ in the limit of the infinite flow rate and the residual $TePixD_D$ in the limit of the zero flow rate. The curves accurately reproduced the observed data over a wide flow-rate range. The value of the excitation rate, k_{exc}, was estimated to be 3.6×10^4 s^{-1} using the rough estimate for l of 40 μm and the reported value of the photoreaction quantum yield, Φ, of 0.29.[12] The value of k_{exc} can also be estimated from the typical value of the flavin molar-extinction coefficient, ca. 8000 M^{-1} cm^{-1}, and the excitation laser power of the present experiment, 500 W/cm^2. Using these values, k_{exc} was estimated to be 3.2×10^4 s^{-1}. The rough concordance between the two values of k_{exc} estimated from different parameters validates the present interpretation that $TePixD_D$ accumulates by rapid circulation. This was also confirmed by the observation that the fluorescence decay under rapid circulation became faster by irradiation of another blue light at the upstream of the circulation (data not shown). Hereafter, the fluorescence dynamics observed with a flow rate of 360 mL/min and with no flow are designated as those of $TePixD_D$ and $TePixD_{red}$, respectively.

The above analysis showed that the fluorescence decay of $TePixD_D$ is expressed by a double-exponential function with time constants of 13.6 and 114 ps. On the other hand, the fluorescence decay of $TePixD_{red}$ is expressed by a single-exponential function with a time constant of 1.37 ps.

B. Femtosecond−Nanosecond Time-Resolved Fluorescence Spectra of TePixD in the Dark-Adapted and Red-Shifted Forms. Figure 3A shows the fluorescence spectra of $TePixD_D$ (solid line) and $TePixD_{red}$ (dashed line). The excitation wavelength was at 430 nm. The spectra of $TePixD_{red}$ shifted toward the long wavelength side reflecting the red shift of the absorption spectrum. The fluorescence signal around 470 nm was larger in $TePixD_{red}$ than in $TePixD_D$. This is probably due to the increased contribution of the Raman scattering of the water molecules around 460 nm in $TePixD_{red}$, in which the fluorescence quantum yield was drastically reduced. Figure 3B and 3C show the decay-associated spectra (DAS) of $TePixD_D$ and $TePixD_{red}$, respectively. The DAS of $TePixD_{red}$ has a more skewed profile in the shorter wavelength side than $TePixD_D$. This probably reflects the Raman scattering of the water. Figure 3B shows that the two DAS components in $TePixD_D$ have almost the same spectral profiles. This is consistent with the fact that the fluorescence dynamics of TePixD is practically monitoring wavelength independent (data not shown). We interpret here that the two decay components in $TePixD_D$ arise from two slightly different conformations around the FAD. Almost the same profiles between the two DAS in Figure 3B indicate that the conformation differences are slight and have little effect on the fluorescence spectrum.

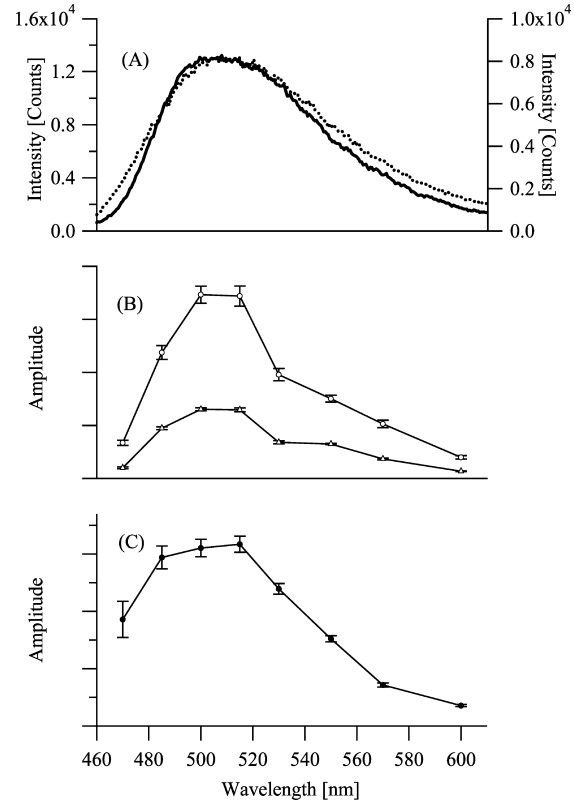

Figure 3. Fluorescence spectra of TePixD in the dark-adapted (solid line, measured by the left axis) and red-shifted (dashed line, measured by the right axis) forms (A). Decay associated spectra of TePixD in the dark-adapted form (B) with decay times of 13.6 (open circles) and 114 ps (open triangles) and in the red-shifted form (C) with a decay time of 1.37 ps (filled circles).

C. Temperature Dependence of the Fluorescence Decay Time of the Dark-Adapted TePixD. Figure 4 shows the temperature dependence of the faster decay time of the fluorescence of $TePixD_D$. The temperature was varied from 10 to 40 °C. The time constant increased slightly as the temperature increased. This is against the Arrhenius law. The solid line shows the fitting to Arrhenius law, giving a small negative activation enthalpy value of -20 ± 31 meV. Since the temperature dependence was negligible compared to the error, we consider here that the fluorescence decay time is practically temperature independent within the accuracy of the present measurement.

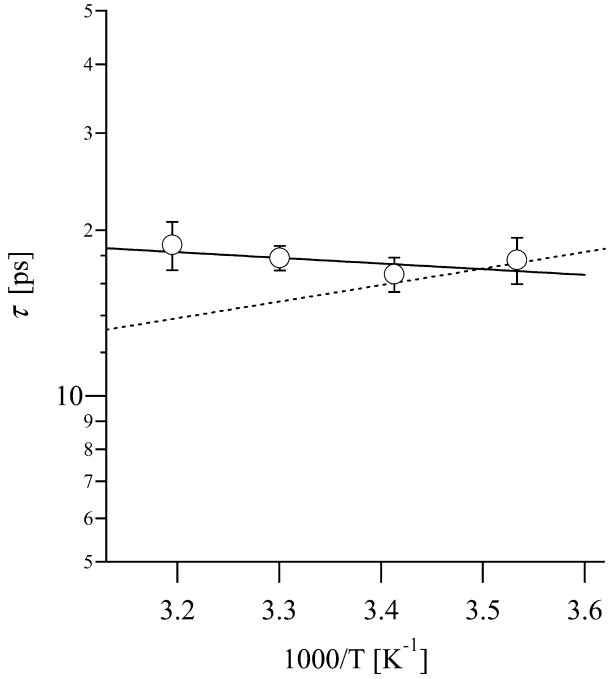

Figure 4. Temperature dependence of the faster time constant in the fluorescence decay at 500 nm of $TePixD_D$. The solid line shows the fitting to the Arrhenius relation. The dashed line is the model curve under the assumption of an activation enthalpy of 58 meV (see text for details).

D. Fluorescence Decays in the Mutants. The fluorescence dynamics of TePixD observed by the up-conversion setup was compared among the mutants in Figure 5. The Tyr8Phe mutant showed an almost nondecaying dynamics in this time region. The streak-camera measurement revealed a single-exponential fluorescence decay with a time constant of 1 ns for Tyr8Phe (data not shown). Thus, Tyr8 plays an essential role in the rapid fluorescence quench in the wild-type TePixD. On the other hand, the mutations at Gln50 showed limited effects on the fluorescence dynamics of TePixD. While the Gln50Ala mutant showed a somewhat faster fluorescence decay than the wild type, the fluorescence decay of Gln50Asn was considerably slower than that of the wild type. The solid lines in Figure 5 are the fitting curves to the sum of three (one for Tyr8Phe) exponentials. The estimated kinetic parameters are listed in Table 1.

IV. Discussion

The fluorescence decays of TePixD in both the dark-adapted and red-shifted forms were observed for the first time with a 200-fs time resolution in the present study. In the mutant TePixD of Tyr8Phe, the fluorescence decay was single exponential and drastically slowed down. This validates the proposed reaction mechanism of BLUF,[20] in which the primary photoreaction is assumed to be the ET reaction from the conserved Tyr to the excited FAD. The fluorescence decay of $TePixD_D$ was double exponential with the dominant component having a time constant of 13.6 ps and the minor one having a 114-ps time constant. The decay of $TePixD_{red}$ was single exponential with a much faster time constant of 1.37 ps. Although we do not have any evidence for the radical-pair formation after the photoreaction of $TePixD_{red}$, we here concluded that its accelerated decay is mainly induced by the enhancement of the ET rate from Tyr8 to the excited FAD. This is reasonable because the rapid fluorescence quenches of many flavoproteins have been shown to come from the ET from the neighboring aromatic residues to the flavin.[34−37]

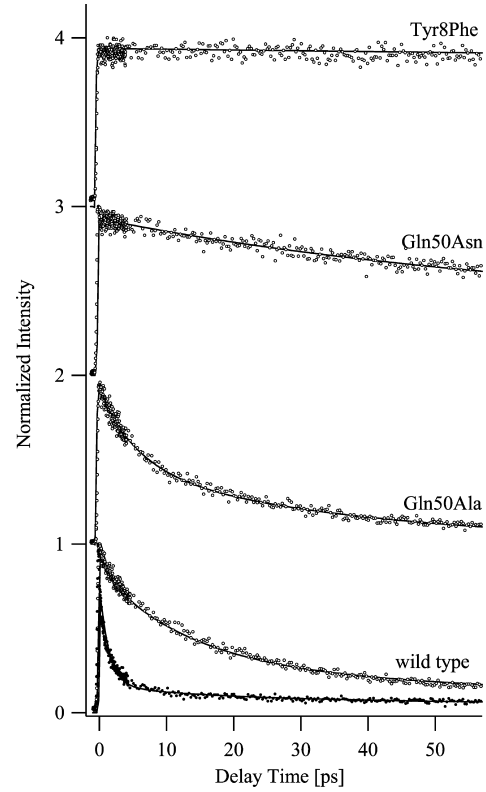

Figure 5. Fluorescence decay curves in the magic-angle configuration of the wild-type, Gln50Ala, Gln50Asn, and Tyr8Phe mutant TePixD at 500 nm. The flow rate was 360 (open circles) and 0 mL/min (wild-type red-shifted form, filled circles).

TABLE 1: Kinetic Parameters of the Fluorescence Decay of TePixD Wild Type in the Dark-Adapted, Product Forms, and TePixD Mutants

sample	τ_1 [ps]	τ_2 [ps]	τ_3 [ps]
WT dark-adapted form	13.6 (71%)	114 (27%)	2000 (2%)
WT red-shifted form	1.37 (98%)	–	2000 (2%)
Gln50Ala	5.6 (50%)	42 (46%)	385 (4%)
Gln50Asn	55 (44%)	225 (50%)	1000 (6%)
Tyr8Phe	–	–	1000 (100%)

The results are basically in line with those of the recent reports for AppA by Toh et al.[25] by using the transient absorption technique and Zirak et al.[32,33] by using time-resolved-fluorescence technique. They showed that the decay of the singlet excited state of FAD in AppA is accelerated more than 10-fold upon light-induced conversion to the red-shifted form. They concluded that the excited FAD of AppA in the red-shifted form enters the forward photoreaction path to rapidly recover the ground-state FAD of the red-shifted form. This ensures the absence of the photoinduced reverse reaction in AppA and seems to be physiologically significant because the efficiency as a light sensor is drastically reduced by the reverse photoreaction in BLUF proteins, which show only slight color differences between the dark-adapted and signaling states.

Both the study by Toh et al. and the present study revealed that BLUF in the dark-adapted form shows a double-exponential decay of the FAD excited state while that in the red-shifted form shows a much faster single-exponential decay. The double-exponential decay in the dark-adapted form suggests the coexistence of two different conformations with different excited-state decay times. The DAS profiles in Figure 3B are practically the same for $TePixD_D$ and $TePixD_{red}$, suggesting that the two conformations have almost the same fluorescence

spectra. The results suggest a rather loose conformation around FAD in the dark-adapted form. The light-induced conversion to the red-shifted form might result in a more rigidly packed conformation around FAD.

The double-exponential decay of the FAD excited state was also observed for Gln50Ala and Gln50Asn mutants. These mutants might have loosely packed conformations around FAD similar to that of the dark-adapted form of the wild type. Both mutants are considered to retain the ability of the primary ET from Tyr8 to FAD. The Gln50Ala and Gln50Asn mutants showed faster and slower fluorescence quenching than the wild type. This result can be explained by the modifications in the Tyr8 conformation induced by the mutations. In the case of the Gln50Ala mutant, the hydrogen bond between Tyr8 and Gln50 was eliminated, as a result of which the conformation of Tyr8 might become more flexible. The enhanced fluctuation in Tyr8 may allow this residue to take the conformation with a shorter distance to FAD, giving a faster ET rate. The larger fluctuation in the conformation of Tyr8 might be reflected in the 50−50 contribution from the faster and slower components in the fluorescence decay process of this mutant (see Table 1). In the Gln50Asn mutant, on the other hand, the Tyr8 conformation with a longer distance to FAD might be preferred due to the hydrogen bond to Asn50, which is shorter than the glutamine residue in the wild type.

Both AppA and TePixD show more than 10-fold acceleration of the decay times of the FAD singlet excited state in the red-shifted form. However, the time scales are significantly different between the two proteins. The fluorescence kinetics of AppA is altered from a double-exponential one with time constants of 90 and 590 ps in the dark-adapted form to a single-exponential one with a time constant of 7 ps in the red-shifted form. All these time constants are much slower than those of TePixD obtained in the present study. Toh et al. reported that the acceleration of the decay time in AppA in the signaling state is mostly due to the enhanced ET rate and partly due to the opening of the direct deactivation path to the FAD ground state.

It is important to note that X-ray crystallographic studies have not shown a wide diversity in the distance between the conserved Tyr (electron donor) and FAD (electron acceptor) among various BLUF proteins. The edge-to-edge distances between the Tyr residue and FAD were estimated to be 3.41 (±0.07) Å in $TePixD_D$,[11] 3.50 (±0.10) Å in SyPixD,[27] 3.23 (±0.16) Å in $AppA_D$, and 3.14 (±0.04) Å in $AppA_{red}$.[28] The distance data shown above were the values averaged over those of the multiple structures determined by X-ray crystallography. The values in parentheses are the standard deviations. Thus, the rate of the primary ET reaction in BLUF proteins does not show any correlation with the donor−acceptor distance. Another example of the correlation absence can be provided. SyPixD shows the primary ET rate of 7 ps in the dark-adapted form[20] while it has a donor−acceptor distance of 3.5 Å,[27] somewhat longer than that of TePixD. It is not clear how similar donor−acceptor distances among various BLUF proteins result in completely different ET rates.

Toh et al. explained the much slower ET rate of AppA in the dark-adapted than in the red-shifted form as being due to inappropriate redox potentials. We can show in the following that the redox-potential adjustment cannot explain the 10-fold acceleration of the ET rate in the red-shifted form in the case of TePixD. According to Marcus's ET theory, the increase in the ET rate can result from either the enhanced electronic factor, V^2, or the optimized free-energy gap, ΔG, between the states before and after ET. The optimized ΔG gives a zero effective activation enthalpy, $H^{\ddagger} = 0$. If the observed increase in the ET rate originates from the modification of the ΔG value, the $H^{\ddagger}$ value is larger in the dark-adapted form than in the red-shifted form. If the ΔG value in $TePixD_{red}$ is assumed to be optimized, we can easily estimate the $H^{\ddagger}$ value in the dark-adapted form to be 58 meV, which gives a 10-fold-slower ET rate in $TePixD_D$ than in $TePixD_{red}$ at room temperature. The dashed line in Figure 4 shows the predicted temperature dependence of the fluorescence decay time using the value $H^{\ddagger} = 58$ meV. The temperature independence of the decay time shown in Figure 4 clearly suggests that the redox potential is almost optimized already in the dark-adapted form. Thus, the acceleration of the primary ET rate in the red-shifted form cannot be explained from the improved redox potentials in the donor and acceptor.

If we consider the primary ET reaction within the framework of Marcus's theory, the enhanced electronic factor V^2 mainly contributes to the accelerated ET rate in the red-shifted form. It has been demonstrated that for the ET reaction in a protein the V^2 value obeys an empirical relation:[38,39]

$$V^2 \propto \exp[-\beta R] \tag{3}$$

where R is the edge-to-edge distance between the donor and acceptor. β is the distance decay factor taking a value of 1.4 $Å^{-1}$. Tanaka et al. analyzed the R dependence of the ET rate of various flavoproteins.[36] According to their analysis, a β value of 1.56 $Å^{-1}$ can be estimated for flavoproteins. Using this β value, we can estimate ca. 1.5-Å shortening of the donor−acceptor distance that gives the 10-fold acceleration of the ET rate.

In the case of $SyPixD_D$, the dominant decay time of the FAD excited state was reported to be 7 ps, which is about 2-fold faster than that of $TePixD_D$ observed in the present study. As described above, the X-ray structures showed that the faster ET rate in $SyPixD_D$ is not attributable to the shorter donor−acceptor distance.[11,27] Possibly, the redox-potential optimization in $TePixD_D$ remains still incomplete, and further optimization might lead to the faster ET rate in $SyPixD_D$. In this case, the effective activation enthalpy in $TePixD_D$ is calculated to be 18 meV, which seems close to the limit of detection of the present study. The acceleration of the primary ET rate in $TePixD_{red}$ may thus come partly from the optimization of the redox potential. In this case the 1.5-Å shortening of the Tyr8−FAD distance is an overestimate. It can be reestimated to be 1.0 Å by considering an incomplete optimization of the redox potentials in the TePixD dark-adapted form.

As shown above, a 1.0−1.5 Å shortening of the donor−acceptor distance upon light-induced conversion to the red-shifted form is estimated from our results. Such a shortening of the Tyr−FAD distance might not be observed in the X-ray diffraction data because conformation changes of a protein after a photoreaction are often restricted in a crystal. Indeed, the absorption spectrum of the AppA crystal showed only a 5-nm red shift upon the photoreaction[28] while that in a solution shows a 10-nm red shift. A red shift by 5 nm is almost the same as that observed in TePixD at 10 K.[12] This was interpreted to be the intermediate state of the forward photoreaction. Chosrowjan et al. suggested that the ET rate in an FMN-binding protein was 20 times slower in a crystalline phase than in a solution.[37] Both NMR and crystallographic studies showed no considerable change in the donor−acceptor distance in a solution and in a crystal. The different ET rate was attributed to the absence of mobile water molecules around the flavin in a crystal.

Recently, Nagai et al. showed that the illumination of $TePixD_{red}$ below 200 K induced a stable radical pair state detected by the electron paramagnetic resonance (EPR) method.[40] They concluded that the EPR signal arose from the dipole−dipole interaction between a neutral flavosemiquinone radical and a neutral tyrosine radical. Their simulation showed that the observed spectral profile could be reproduced only when they presumed a 2.2-Å-shorter Tyr8−FAD distance than that determined by X-ray crystallography. The observed radical pair state was not exactly the red-shifted form, but was produced by illumination to the red-shifted form at low temperatures. The signal was detected by illumination even at 10 K, where a large conformation change should be suppressed. This suggests that the Tyr8−FAD distance shortens before the illumination, in the red-shifted form. The results are consistent with the present conclusion predicting the shortening of the Tyr8−FAD distance in the red-shifted form.

So far, we have discussed the primary ET rate in various BLUF proteins within the framework of Marcus's ET theory. We should consider the other mechanisms that modify the ET rate without any change in the donor−acceptor distance. Recently, Sadeghian et al. proposed that the primary light-induced reaction in BLUF corresponds to the charge-transfer transition to the zwitterionic radical-pair state via the conical intersection. However, it seems unlikely that the conical intersection is the key mechanism in the primary photochemistry of BLUF in the dark-adapted form for the following reason. An excited-state deactivation via the conical intersection is considered to take place within a single cycle of the molecular vibration. Thus, the deactivation time generally ranges from subpicoseconds to several picoseconds.[41] This seems incompatible with the present observation. We cannot exclude the possibility that the enhanced ET rate in $TePixD_{red}$ is due to the conical intersection mechanism.

V. Concluding Remarks

The fluorescence decay times of both $TePixD_D$ and $TePixD_{red}$ could be unequivocally determined for the first time in the present study. It was shown that the excited state of FAD decays 10-fold faster in the red-shifted form than in the dark-adapted form. The fluorescence decay was double exponential in the dark-adapted form, suggesting heterogeneity in the conformation around FAD. According to the results, the following scenario is inferred: the photoreaction to the red-shifted form results in a more rigid and compact conformation around FAD. In that conformation, the Tyr8−FAD distance is shortened by 1.0−1.5 Å, and the fluorescence decay of FAD is accelerated 10-fold by the shortening. Such a shortening might escape detection in the X-ray diffraction data. However, it might reflect a large conformation change that is essential for signal transduction.

Acknowledgment. The work was supported in part by Grants-in-Aid for Scientific Research (No. 17750010), the 21st COE program for "The Origin of the Universe and Matter" from the Japanese Ministry of Education, Science, Sports, and Culture (MEXT), and the Japan Society for the Promotion of Science.

References and Notes

(1) Masuda, S.; Bauer, C. E. *Cell* **2002**, *110*, 613.
(2) Kennis, J. T. M.; Crosson, S.; Gauden, M.; van Stokkum, I. H. M.; Moffat, K.; van Grondelle, R. *Biochemistry* **2003**, *42*, 3385.
(3) Giovani, B.; Byrdin, M.; Ahmad, M.; Brettel, K. *Nat. Struct. Biol.* **2003**, *10*, 489.
(4) Kim, S. T.; Heelis, P. F.; Okamura, T.; Hirata, Y.; Mataga, N.; Sancer, A. *Biochemistry* **1991**, *30*, 11262.
(5) Kao, Y. T.; Saxena, C.; Wang, L. J.; Sancar, A.; Zhong, D. P. *Proc. Natl. Acad. Sci. U.S.A.* **2005**, *102*, 16128.
(6) Gomelsky, M.; Kaplan, S. *J. Biol. Chem.* **1998**, *273*, 35319.
(7) Laan, W.; van der Horst, M. A.; van Stokkum, I. H. M.; Hellingwerf, K. J. *Photochem. Photobiol.* **2003**, *78*, 290.
(8) Masuda, S.; Hasegawa, K.; Ishii, A.; Ono, T. *Biochemistry* **2004**, *43*, 5304.
(9) Rajagopal, S.; Key, J. M.; Purcell, E. B.; Boerema, D. J.; Moffat, K. *Photochem. Photobiol.* **2004**, *80*, 542.
(10) Masuda, S.; Hasegawa, K.; Ono, T. *Biochemistry* **2005**, *44*, 1215.
(11) Kita, A.; Okajima, K.; Morimoto, Y.; Ikeuchi, M.; Miki, K. *J. Mol. Biol.* **2005**, *349*, 1.
(12) Fukushima, Y.; Okajima, K.; Shibata, Y.; Ikeuchi, M.; Itoh, S. *Biochemistry* **2005**, *44*, 5149.
(13) Zirak, P.; Penzkofer, A.; Lehmpfuhl, C.; Mathes, T.; Hegemann, P. *J. Photochem. Photobiol., B* **2007**, *86*, 22.
(14) Unno, M.; Sano, R.; Masuda, S.; Ono, T.; Yamauchi, S. *J. Phys. Chem. B* **2005**, *109*, 12620.
(15) Unno, M.; Masuda, S.; Ono, T.; Yamauchi, S. *J. Am. Chem. Soc.* **2006**, *128*, 5638.
(16) Okajima, K.; Fukushima, Y.; Suzuki, H.; Kita, A.; Ochiai, Y.; Katayama, M.; Shibata, Y.; Miki, K.; Noguchi, T.; Itoh, S.; Ikeuchi, M. *J. Mol. Biol.* **2006**, *363*, 10.
(17) Kottke, T.; Heberle, J.; Hehn, D.; Dick, B.; Hegemann, P. *Biophys. J.* **2003**, *84*, 1192.
(18) Crosson, S.; Rajagopal, S.; Moffat, K. *Biochemistry* **2003**, *42*, 2.
(19) Okajima, K.; Yoshihara, S.; Fukushima, Y.; Geng, X. X.; Katayama, M.; Higashi, S.; Watanabe, M.; Sato, S.; Tabata, S.; Shibata, Y.; Itoh, S.; Ikeuchi, M. *J. Biochem.* **2005**, *137*, 741.
(20) Gauden, M.; van Stokkum, I. H. M.; Key, J. M.; Lührs, D. Ch.; van Grondelle, R.; Hegemann, P.; Kennis, J. T. M. *Proc. Natl. Acad. Sci. U.S.A.* **2006**, *103*, 10895.
(21) Fukushima, Y.; Murai, Y.; Okajima, K.; Ikeuchi, M.; Itoh, S. *Biochemistry* **2008**, *47*, 660.
(22) Sadeghian, K.; Bocola, M.; Schütz, M. *J. Am. Chem. Soc.* **2008**, *130*, 12501.
(23) Domratcheva, T.; Grigorenko, B. L.; Schlichting, I.; Nemukhin, V. *Biophys. J.* **2008**, *94*, 3872.
(24) Gauden, M.; Yeremenko, S.; Laan, W.; van Stokkum, I. H.; Ihalainen, J. A.; van Grondelle, R.; Hellingwerf, K. J.; Kennis, J. T. M. *Biochemistry* **2005**, *44*, 3653.
(25) Toh, K. C.; van Stokkum, I. H. M.; Hendriks, J.; Alexandre, M. T. A.; Arents, J. C.; Perez, M. A.; van Grondelle, R.; Hellingwerf, K. J.; Kennis, J. T. M. *Biophys. J.* **2008**, *95*, 312.
(26) Anderson, S.; Dragnea, V.; Masuda, S.; Ybe, J.; Moffat, K.; Bauer, C. *Biochemistry* **2005**, *44*, 7998.
(27) Yuan, H.; Anderson, S.; Masuda, S.; Dragnea, V.; Moffat, K.; Bauer, C. *Biochemistry* **2006**, *45*, 12687.
(28) Jung, A.; Reinstein, J.; Domratcheva, T.; Shoeman, R. L.; Schlichting, I. *J. Mol. Biol.* **2006**, *362*, 717.
(29) Marcus, R. A.; Sutin, N. *Biochim. Biophys. Acta* **1985**, *811*, 265.
(30) Dragnea, V.; Waegele, M.; Balascuta, S.; Bauer, C.; Dragnea, B. *Biochemistry* **2005**, *44*, 15978.
(31) Gauden, M.; Grinstead, J. S.; Laan, W.; van Stokkum, I. H. M.; Avila-Perez, M.; Toh, K. C.; Boelens, R.; Kaptein, R.; van Grondelle, R.; Hellingwerf, K. J.; Kennis, J. T. M. *Biochemistry* **2007**, *46*, 7405.
(32) Zirak, P.; Penzkofer, A.; Schiereis, T.; Hegemann, P.; Jung, A.; Schlichting, I. *Chem. Phys.* **2005**, *315*, 142.
(33) Zirak, P.; Penzkofer, A.; Schiereis, T.; Hegemann, P.; Mathes, T. *Chem. Phys.* **2007**, *335*, 15.
(34) Mataga, N.; Chosrowjan, H.; Shibata, Y.; Tanaka, F.; Nishina, Y.; Shiga, K. *J. Phys. Chem. B* **2000**, *104*, 10667.
(35) Zhong, D. P.; Zewail, A. H. *Proc. Natl. Acad. Sci. U.S.A.* **2001**, *98*, 11867.
(36) Tanaka, F.; Chosrowjan, H.; Taniguchi, S.; Mataga, N.; Sato, K.; Nishina, Y.; Shiga, K. *J. Phys. Chem. B* **2007**, *111*, 5694.
(37) Chosrowjan, H.; Taniguchi, S.; Mataga, N.; Tanaka, F.; Todoroki, D.; Kitamura, M. *J. Phys. Chem. B* **2007**, *111*, 8695.
(38) Moser, C. C.; Dutton, P. L. *Biochim. Biophys. Acta* **1992**, *1101*, 171.
(39) Page, C. C.; Moser, C. C.; Chen, X.; Dutton, P. L. *Nature* **1999**, *402*, 47.
(40) Nagai, H.; Fukushima, Y.; Okajima, K.; Ikeuchi, M.; Mino, H. *Biochemistry* **2008**, *47*, 12574.
(41) Migani, A.; Robb, M. A.; Olivucci, M. *J. Am. Chem. Soc.* **2003**, *125*, 2804.

JP901631B